Plant Cell Rep (2010) 29:735–746
DOI 10.1007/s00299-010-0860-6

ORIGINAL PAPER

Molecular and genetic characterization of novel *S-RNases* from a natural population of *Nicotiana alata*

Juan A. Roldán · Rodrigo Quiroga · Ariel Goldraij

Received: 23 December 2009 / Revised: 12 April 2010 / Accepted: 15 April 2010 / Published online: 5 May 2010

Abstract Self-incompatibility in the Solanaceae is mediated by *S-RNase* alleles expressed in the style, which confer specificity for pollen recognition. *Nicotiana alata* has been successfully used as an experimental model to elucidate cellular and molecular aspects of S-RNase-based self-incompatibility in Solanaceae. However, *S-RNase* alleles of this species have not been surveyed from natural populations and consequently the *S*-haplotype diversity is poorly known. Here the molecular and functional characterization of seven *S-RNase* candidate sequences, identified from a natural population of *N. alata*, are reported. Six of these candidates, S_5, S_{27}, S_{70}, S_{75}, S_{107}, and S_{210}, showed plant-specific amplification in the natural population and style-specific expression, which increased gradually during bud maturation, consistent with the reported *S-RNase* expression. In contrast, the S_{63} ribonuclease was present in all plants examined and was ubiquitously expressed in different organs and bud developmental stages. Genetic segregation analysis demonstrated that S_{27}, S_{70}, S_{75}, S_{107}, and S_{210} alleles were fully functional novel *S-RNases*, while S_5 and S_{63} resulted to be *non-S-RNases*, although with a clearly distinct pattern of expression. These results reveal the importance of performing functional analysis in studies of *S*-RNase allelic diversity. Comparative phylogenetic analysis of six species of Solanaceae showed that *N. alata S-RNases* were included in eight transgeneric *S*-lineages. Phylogenetic pattern obtained from the inclusion of the novel *S-RNase* alleles confirms that *N. alata* represents a broad sample of the allelic variation at the *S*-locus of the Solanaceae.

Keywords Natural populations · *Nicotiana alata* · Self-incompatibility · *S*-Haplotype · S-RNase · Transgeneric *S*-lineages

Communicated by R. Schmidt.

Electronic supplementary material The online version of this article (doi:10.1007/s00299-010-0860-6) contains supplementary material, which is available to authorized users.

J. A. Roldán · R. Quiroga · A. Goldraij (✉)
Departamento de Química Biológica, Facultad de Ciencias Químicas, Centro de Investigaciones en Química Biológica de Córdoba (CIQUIBIC, UNC–CONICET), Universidad Nacional de Córdoba, Haya de la Torre y Medina Allende, Ciudad Universitaria, X5000HUA Córdoba, Argentina
e-mail: arielg@fcq.unc.edu.ar

Introduction

Self-incompatibility (SI) is a prezygotic reproductive barrier based on the recognition and subsequent rejection of self or genetically related pollen. More than half of the approximately 250,000 angiosperm species display some form of SI (de Nettancourt 2001), thus there is apparently considerable pressure to prevent inbreeding and maintain genetic diversity. SI is genetically determined by the *S*-locus, which controls the specificity of pollen–pistil recognition. The *S*-locus has at least two genes encoding for male and female specificity factors, selectively expressed in pollen and pistil, respectively. Both genes are multiallelic and they are inherited as a segregating unit; therefore, each allelic pair defines a haplotype of SI. In Solanaceae and other families, the SI system is gametophytic (GSI); the compatibility phenotype of a pollen tube growing through the style is determined by its own haploid genotype. Pollen rejection occurs when the *S*-haplotype expressed by pollen matches any of the *S*-haplotypes expressed in the diploid pistil.

Seminal research on molecular basis of Solanaceae SI was conducted mainly on *Nicotiana*, *Petunia,* and *Solanum* as experimental models. S-RNase was found to be the factor conferring pistil specificity for pollen recognition (McClure et al. 1989; Lee et al. 1994; Murfett et al. 1994) and the cytotoxic agent in the pollen rejection process, by degradation of pollen tube RNA (McClure et al. 1990; Huang et al. 1994). Five conserved domains and two hypervariable domains were identified in the primary structure of solanaceous S-RNases, the latter playing a key role in the determination of female specificity and the interaction with the pollen counterpart (Ioerger et al. 1991; Matton et al. 1997). On the other hand, the gene encoding the pollen specificity factor, the SLF (S-locus F-Box) protein, has been identified and cloned in *Petunia* (Sijacic et al. 2004) and recently, several *SLF* orthologue candidates in *Nicotiana* were reported (Wheeler and Newbigin 2007). S-RNase enters both compatible and incompatible pollen tubes to interact with SLF (Luu et al. 2000; Goldraij et al. 2006), although the nature of this interaction is still unknown.

In contrast with the remarkable progress made in the last 20 years at the cellular, molecular, and biochemical levels, our knowledge about SI in natural populations of *Nicotiana* is quite different from that in *Petunia* and *Solanum*. While in *Petunia* and *Solanum S*-allele variation is well-studied from natural populations, to our knowledge there are no reports about similar studies in *Nicotiana*. Natural populations are useful to investigate the allelic diversity of self-incompatible species because they usually contain a large number of *S*-alleles. These *S*-alleles are subjected to negative frequency-dependent selection which greatly increases the persistence of polymorphism at the *S*-locus. PCR techniques based on the conserved domains of *S*-RNases offer a simple and efficient approach to examine allelic variants of *S-RNases*. Pioneering research following this approach was described in *Solanum carolinense* (Richman et al. 1995). Natural populations of *Petunia* and other *Solanum* species were also surveyed and several new *S-RNase* alleles have been identified from these analyses. For example, 21 *S-RNase* alleles were found in *Petunia inflata* (Wang et al. 2001), while in *Solanum chilense*, 34 *S-RNase* alleles were recently reported (Igic et al. 2007). Natural populations of other solanaceous genera such as *Physalis* (Richman et al. 1996; Lu 2006), *Witheringia* (Stone and Pierce 2005) and *Lycium* (Savage and Miller 2006; Miller et al. 2008) were also examined and the number of identified *S-RNase* alleles ranged between 21 and 36. Besides the large diversity of *S*-alleles, wild populations often show marked individual differences in terms of the robustness of the SI response. In both *Petunia* and *Solanum*, natural populations of mixed, self-incompatible, and self-compatible individuals have been described (Tsukamoto et al. 1999, 2003a; Kokubun et al. 2006; Mena-Alí and Stephenson 2007). Self-compatible (SC) individuals of otherwise self-incompatible species constitute a valuable potential source for revealing the complex molecular machinery participating in the pollen rejection of S-RNase-based SI (McClure 2008).

In this paper, we focus on the self-incompatible species *Nicotiana alata* (Goodspeed 1954), a model system both in early genetic studies of SI as well as in the modern biochemical analysis of SI (reviewed in McClure 2009). The mating system, the pollen rejection mechanisms and the pollination biology between this species and its relatives of section Alatae have been extensively studied (Pandey 1979; Murfett et al. 1996; McClure et al. 2000; Ippolito et al. 2004; Lee et al. 2008). However, given the lack of studies about *S*-allelic diversity in natural populations of *N. alata*, the number of reported *S-RNase* alleles in this species is quite small compared to other Solanaceae. Some *S-RNase* accessions of *N. alata* have been annotated with different codes (i.e., S_7- and S_{c10}-*RNase*) despite their identical deduced amino acid sequences. Other accessions correspond to putative S-RNases, without clear confirmation of their functional role as *S*-alleles, i.e., MS1 and MS2 (Kuroda et al. 1994). Given the very high similarity in primary structural traits, it cannot be ruled out that putative *S-RNases* not subjected to functional assays, are in fact *S-like-RNases* or relic *S-RNases* not involved in SI (Green 1994; Golz et al. 1998). These genes have been reported in pistils of both self-compatible and self-incompatible species of many plant families (Green 1994; Kao and Tsukamoto 2004), including *N. alata* (Dodds et al. 1996). Sequencing therefore is not sufficient to confirm conclusively the SI function of putative *S-RNase* allele sequences and thus, functionality assays are critically important to identify clearly functional *S-RNases* (Igic et al. 2007).

As part of the analysis of natural variation in the *S*-locus of Solanaceae, the aim of this work was to identify and characterize novel *S-RNase* alleles of self-incompatible *N. alata* from a natural population located in northeastern Argentina. Using an RT-PCR approach, we recovered seven novel *S-RNase* candidate sequences. By allele-specific amplification, we examined the expression profile of these *S-RNase* candidates in a sample of the natural population, in different tissues and pistil developmental stages, and also in other plant populations including SI and SC genotypes. We also performed controlled crosses to establish whether the novel ribonuclease sequences were functional as *S*-alleles. Finally, phylogenetic analysis was used to determine the extent of *S-RNase* polymorphism in *N. alata* and the distribution of novel *S-RNases* among the different *S*-lineages of the Solanaceae. Five novel functional *S-RNases*, identified from the natural population,

are reported. Two *non-S-RNases*, which exhibited a contrastable expression pattern in different plants and tissues, were also characterized. Interestingly one of these *non-S-RNases* appears to be present in SC *Nicotiana longiflora* and a SC accession of *N. alata.*

Materials and methods

Plant material and growth conditions

The natural population of *N. alata* studied in this work was designated NaM; it was collected in Province of Misiones, Argentina, on the coast of Paraná River, approximately 300 m from the confluence of Paraná and Iguazú rivers (25°35′50″S, 54°35′34″W) on 26 November 2006. The population occupied an area of approximately 5,000 m^2 and consisted of 15 isolated plants established in a stony soil, poorly covered with vegetation. Seeds were collected randomly from capsules, mixed and stored at 4°C until use. Plants were grown in a greenhouse at 28°C with 16/8 h light/dark period. NaM-1 to NaM-8 individuals were selected at random from NaM population seeds. NaM-9 to NaM-12 derived from a screening of NaM population seedlings by allele-specific PCR, to select plants not harboring the S_5*-RNase*. NaM-t1 and NaM-t2 individuals were tester plants, derived from the cross of NaM-5 × $S_{c10}S_{c10}$ (the latter being obtained from bud-selfing of NaM-7). All plants consistently failed to set fruits upon selfing, except NaM-1 and NaM-8 that occasionally set small capsules. The SI response of these two plants will be detailed elsewhere.

The presence of *S-RNase* candidate genes was tested in *N. longiflora*, a laboratory stock of *N. alata* and a SC accession of *N. alata*. Seeds of *N. longiflora*, a self-compatible member of section Alatae (Goodspeed 1954) were collected from a natural population in Ciudad Universitaria, Córdoba, Argentina (31°26′18″S, 64°11′23″W). A laboratory stock of the *N. alata* genotypes $S_{c10}S_{105}$, $S_{c10}S_{a2}$, and $S_{105}S_{a2}$ was obtained by crossing homozygous lines $S_{c10}S_{c10}$, $S_{105}S_{105}$ and $S_{a2}S_{a2}$ previously described (Murfett et al. 1996; McClure et al. 1999). SC *N. alata* cv Breakthrough (BT) was obtained from Thompson and Morgan, Jackson, NJ, USA. Plants were grown at conditions described for *N. alata*. At least, two individuals of each species or genotype were selected for the experiments of Fig. 2b, c.

Nucleic acid extraction

Genomic DNA was purified from leaves by phenolic extraction and ethanol precipitation of DNA or using GenElute™ Plant Genomic DNA Miniprep kit (Sigma, St Louis, MO). Total RNA was extracted from styles (including the stigma) according to McClure et al. (1990).

DNA extracts were used to determine progeny genotypes in *S*-functionality assays (see below). DNA was extracted from small pieces of plantlet leaves by slight homogenization with a plastic pestle in 0.2 ml of 0.2 M Tris–ClH pH 8 containing 0.25 M NaCl, 0.02 M EDTA, and 0.5% w/v SDS. After heating at 65°C for 5 min, supernatant was precipitated successively with isopropanol and 70% ethanol and resuspended in sterile water. 0.4–2 µl of leaf extract was used as template in a 20 µl of PCR reactions as indicated below.

PCR, cloning, and sequencing of *S-RNase* candidates

S-RNase candidates from *N. alata* styles were amplified using degenerate primers based on conserved domains C1 and C5 (Ioerger et al. 1991), which amplified a single cDNA fragment of expected size. Further characterization of this fragment was performed using additional degenerate primers, based on C2 and C4 conserved domains (Supplementary Fig. S1). All sequences of degenerate and allele-specific primers are detailed in Supplementary Table S1.

Genomic PCR was performed in 20-µl reactions containing 0.4 units of GoTaq® Flexi DNA polymerase (Promega, Madison WN), GreenGoTaq Flexi buffer®, 1.5 mM $MgCl_2$, 0.2 mM dNTPS, and 12.5–33 pg of DNA. Primers were used at 0.4 and 1.2 µM for specific and degenerate primers, respectively. The reaction was incubated at 95°C for 5 min and then by 40 cycles of 1 min at 94°C, 45 s at the annealing temperature indicated in supplementary Table S1, and 1 min at 72°C, followed by a final extension step of 5 min at 72°C.

For RT-PCR amplification, 1 µg of total RNA and 5.5 µM oligo $(dT)_{15}$ were incubated for 5 min at 70°C, chilled in ice water for 5 min, and mixed with 6 mM $MgCl_2$, 0.5 mM dNTPs, 1 µl of ImProm-II™ Reverse Transcriptase and ImProm-II™ buffer (Promega, Madison WN) in a final volume of 20 µl. Single-stranded cDNA synthesis was performed for 1 h at 42°C, according to manufacturer's instructions. A 2 µl aliquot of cDNA synthesis reaction was used as template for PCR amplification, following the procedure indicated above for genomic PCR. Amplified fragments were analyzed on agarose gels, purified and cloned into pGEM-Teasy vector (Promega, Madison WN). Twenty to thirty recombinant plasmids were analyzed by restriction enzyme digestion or allele-specific PCR. All different types of plasmid identified were sequenced with standard SP6 or T7 promoter primers (Macrogen Inc, MD, USA). For each type of clone identified, both DNA strands from two or more plasmids were sequenced.

For RT-PCR analysis of *S-RNase* transcripts, total RNA was isolated from stigma/style, pollen, sepals, petals, and from styles of different developmental stages. Linearity of allele-specific PCR amplification was assessed with Gel-Pro™ Analyzer 3.0. Actin was used as positive amplification control. Sequence data of novel genes described in this work have been deposited with the GenBank Data Libraries under accession nos. GQ375150–GQ375155 and GQ850520.

Functionality assays of novel *S-RNase* candidates

S-functionality was established by crossing plants sharing the tested *S*-allele candidate (half-compatible crosses) and subsequent genotyping of the progeny by allele-specific PCR on DNA extracts. Flowers were emasculated 2 days before anthesis and heavily pollinated within 24 h after anthesis. In half-compatible crosses, if the alleles tested were functional in SI, they are expected to be present in 50% of the progeny, due to the exclusive maternal contribution (assuming full viability of gametes and equal probability of segregation). However, if the shared alleles were not functional in SI, their proportion in the progeny would be higher, reflecting paternal contribution. Likewise, all of the progeny of half-compatible crosses bear the single compatible paternal allele. For instance, in the cross $BC \times AB$, where *A*, *B*, and *C* are *S*-alleles, if *B* is a fully functional SI allele in both pollen and style, then the cross will be half-compatible and the allele *A* will represent the single pollen contribution to the progeny, *AB* and *AC*. Using this strategy, functional and non-functional *S*-haplotypes were recently identified in species with S-RNase-based SI (Hauck et al. 2006; Igic et al. 2007; Tsukamoto et al. 2008).

Protein alignment and phylogenetic analysis

S-RNase nucleotide sequences spanning the region between the conserved domains C2–C5 (Ioerger et al. 1991) were translated into amino acid sequences, aligned with *ClustalX* (Thompson et al. 1997), back-translated to a nucleotide alignment and manually adjusted to ensure proper alignment of conserved sites in solanaceous S-RNases. Percentage of pairwise amino acid identity were determined using Megalign™ 5.00 (DNASTAR). Gene trees were reconstructed using Bayesian inference (BI) and maximum-likelihood (ML) methods with MrBayes v3.2 (Ronquist and Huelsenbeck 2003) and RaxML 7.04 (Stamatakis 2006), respectively. For determining Bayesian inference phylogeny, four parallel Monte-Carlo Markov Chains (MCMC) were run for 10 million generations to search tree space, with a sample frequency of 100 generations. The General Time-Reversible (GTR) model of substitution was used, approximating the rate of variation across sites by using four discrete gamma categories. A consensus 50% majority rule tree was constructed with MrBayes subprogram "Sumt", discarding the initial 25% of the trees generated in each run as burn-in. Stationarity was suggested by average standard deviation of split frequencies remaining below 0.01 after 6.5 million generations, and potential scale reduction factor (PSRF) values for all parameters ranging between 1.000 and 1.003. ML phylogeny was estimated using the GTR+CAT approximation (Stamatakis et al. 2008) to model among-site rate variation, using a maximum parsimony starting tree to perform 1,000 rapid-bootstraps, and the GTR model with 4 discrete gamma categories to perform a thorough ML search for the best scoring tree (traditional non-parametric bootstrapping was performed with very similar results). Tree topology from the best scoring ML tree and the consensus BI tree proved to be very similar. Posterior probabilities for clades from the consensus BI tree were mapped onto the best scoring ML tree. Five species in addition to *N. alata* were included in the phylogenetic analysis, representing both broad (*Solanum chilense*, *Lycium parishii*, *Petunia inflata*) and restricted (*Physalis longifolia*, *Witheringia solanacea*) distributions of *S-RNase* alleles in *S*-lineages. The number of transgeneric (TG) lineages was determined for *N. alata S-RNases* considering a TG lineage as the most recent node including alleles from more than one species (Savage and Miller 2006). A total allele set of 154 individual sequences was used for generating a phylogenetic tree, in which the S_3*-RNase* from *Antirrhinum hispanicum* was assigned as the outgroup. (See Supplementary File S1 for the accession numbers of the sequences included in the phylogenetic analysis.) The phylogenetic tree comparing relic *S-RNases*, *S-RNases* (both from the Solanaceae, Plantaginaceae, and Rosaceae) and *S-like RNases* is a BI tree built as described above, except for MCMC run length, which was 3 million generations. Ribonuclease T2 from *Aspergillus oryzae* was assigned as the outgroup.

Results

Identification of putative *S-RNases* from a natural population of *Nicotiana alata*

C1–C5 cDNA fragments (Supplementary Table S1; Supplementary Fig. S1) amplified from styles of 12 plants of the natural population of *N. alata* were cloned, classified by restriction digests, and sequenced. Three of these sequences were more than 99% identical to S_{c10}-, S_2-, and S_6*-RNases*, which were previously characterized as functional SI alleles (Anderson et al. 1989; Murfett et al. 1996).

A fourth putative *S-RNase* sequence, designated here S_{63}, was almost identical to ribonuclease MS1 described by Kuroda et al. (1994). Six additional putative *S-RNase* sequences, not previously reported and denoted here as S_5-, S_{27}-, S_{70}-, S_{75}-, S_{107}-, and S_{210}-*RNase* candidates, were also recovered from the 12 plants analyzed. In some plants only one *S-RNase* candidate of the two expected for the GSI locus was identified, while in other plants, three or even four different *S-RNases* candidates were identified (Supplementary Table S2).

The cDNA of the S_{c10}-*RNase* allele was used as reference in the alignment of the deduced amino acid sequences of the C1–C5 fragments amplified from the novel *S-RNase* candidates (Fig. 1). The C1–C5 fragment (without including C1f and C5r primer sequences) accounts for approximately 70% of the full size of solanaceous S-RNases (Ioerger et al. 1991). All sequences showed the expected conserved domains C2, C3, and C4 as well as the hypervariable regions HVa and HVb, located between C2 and C3 domains. They also exhibited other typical traits of S-RNase primary structure, such as the glycosylation site in C2, the five conserved cysteine sites included between the C1 and C5 domains, and the histidine residues, included in the C2 and C3 domains, involved in the catalytic activity of T2-type ribonucleases. Except for the pairs S_{70}/S_{63} and S_5/S_{75}, which showed the highest amino acid pairwise identity (81 and 83%, respectively), the amino acid identity among the novel S-RNase candidates ranged from 40 to 58%. This high degree of allelic sequence diversity was similar to values previously found among solanaceous S-RNases (typically 50% of amino acid pairwise identity) (McClure et al. 2000; Kao and Tsukamoto 2004). In the pair S_{70}/S_{63} most non-conservative differences were concentrated in HVa and HVb regions while in the pair S_5/S_{75}, non-conservative changes were distributed uniformly in the C1–C5 sequence, albeit with a small concentration in the HVa region. A pairwise alignment of S-RNase candidates S_{70}/S_{63} and S_5/S_{75} is shown in Supplementary Fig. S2. Percentage of pairwise amino acid identity of all novel S-RNase candidates is shown in Table S3.

Specificity of *S-RNase* candidates expression

To determine whether *S-RNase* candidates showed the typical characteristics of *S-RNases*, the expression specificity of each candidate in different plants of the NaM population was assayed by RT-PCR. Then, the relative expression of *S-RNase* candidate sequences was examined in different tissues and stages of style maturity. Finally, controlled crosses to test whether novel alleles were associated with the SI phenotype were performed. In all these experiments, *S-RNase* candidates were tested in parallel to the S_{c10}-*RNase*, a well-characterized *S*-allele with a robust SI phenotype (Murfett et al. 1994), used here as a functional *S-RNase* reference.

Allele-specific primers based on nucleotide sequences of *S-RNase* hypervariable regions HVa and HVb (Supplementary Table S1), amplified single fragments of the expected sizes from cDNA of the 12 NaM individuals (Fig. 2a). As expected, RT-PCR with the S_{c10}-*RNase* primer set revealed a specific amplification product in plants 2 and 7, consistent with results shown in Supplementary Table S2. Similarly, amplification with the S_2- and S_6-*RNase* primer sets rendered a band only in plants 4 and 9, respectively. Likewise, RT-PCR with specific primers of putative S_{70}-, S_{75}-, S_{27}-, S_{107}-, S_{210}-, *and* S_5-, *RNases* amplified the corresponding products in the expected plants (Supplementary Table S2), and also revealed the presence of these alleles in other plants. These results confirm that the aforementioned *S-RNase* candidates are plant specific and suggest that they could represent *S-RNase* genes. By contrast, the amplification product of S_{63} was present in all 12 plants examined indicating that this ribonuclease was not a functional *S-RNase*. (Supplementary Fig. S3A).

To gain more insight about the relationship of novel *S-RNase* candidates with the SI system, their expression was also tested in a well-genotyped laboratory stock of *N. alata* and in a SC species *N. longiflora* (Fig. 2b, c). As expected, S_{c10}-*RNase* was detected in $S_{c10}S_{105}$ and $S_{c10}S_{a2}$ genotypes. Consistent with its ubiquity, the S_{63} sequence was detected in the three *S*-genotypes assayed, confirming that it is a ribonuclease not involved in *S*-specificity. Moreover, S_{63} was also amplified in both SC *N. longiflora* and also in a self-compatible accession of *N. alata* (cultivar Breakthrough), which does not express an *S-RNase* (McClure et al. 1999) (Fig. 2c). In contrast, none of the other novel *S-RNase* candidates assayed were detected in the three *N. alata* genotypes analyzed (Fig. 2b; Supplementary Fig. S3B). The S_{c10}-*RNase* and the S_5-, and S_{75}-*RNase* candidates were not detected in any of the two SC genotypes assayed in Fig. 2c (results not shown).

To further characterize putative *S-RNases*, tissue specificity and temporal expression was investigated by RT-PCR analysis of transcripts. The relative expression pattern in different organs of S_5-, S_{107}, and S_{70}-*RNase* candidates showed close resemblance to the S_{c10}-*RNase* pattern, rendering the expected amplification product in styles but not in other floral tissues or leaves (Fig. 3a). By contrast, transcripts of non-S_{63}-*RNase* were detected in all organs analyzed, albeit amplification in style, petals, and sepals was higher than in pollen and leaf. Temporal expression of *S-RNase* candidates was also analyzed in developing styles. Similar to the tissue-specific pattern, the expression of the S_5- S_{70}, and S_{107}-*RNase* candidates paralleled the pattern exhibited by S_{c10}-*RNase* (Fig. 3b). The RT-PCR amplification of these *S-RNase* candidates was not detected at the

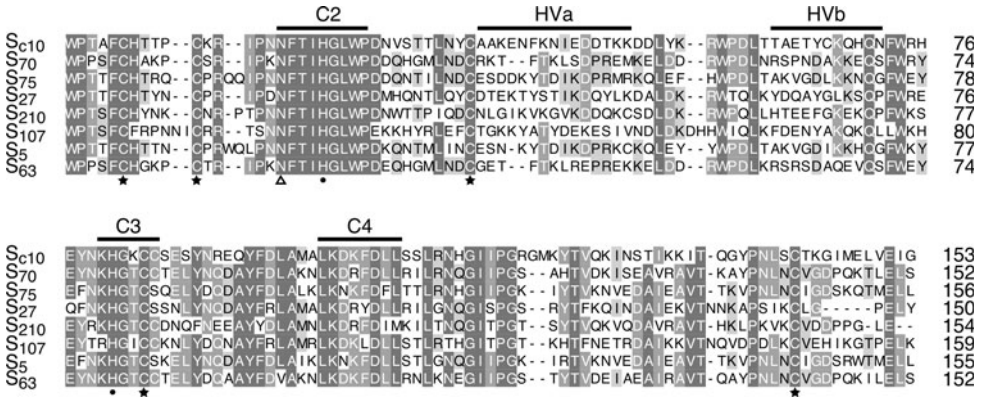

Fig. 1 Deduced amino acid alignment of S-RNase candidates identified from a natural population of *Nicotiana alata*. The fragments aligned were amplified with C1f-C5r primer set detailed in Table S1. The S_{c10}-RNase was used as reference. Amino acids are *shaded* according to percentage agreement. Three conserved domains (C2, C3 and C4) and the two hypervariable regions (HVa and HVb) of S-RNases from Solanaceae are indicated by *solid lines*. Other common S-RNase traits like conserved cysteines (*stars*), histidine residues involved in catalytic activity (*black dots*), and glycosylation site (*black triangle*), are marked

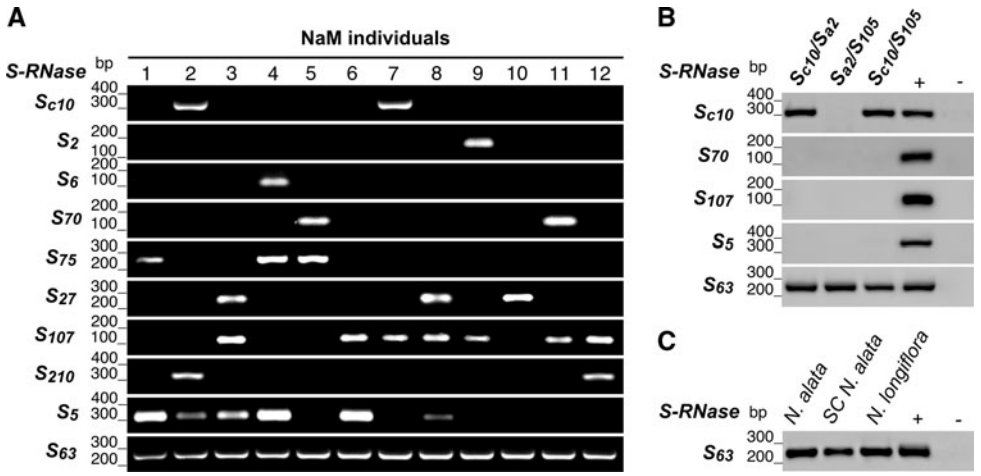

Fig. 2 Allele-specific PCR of *Nicotiana alata S-RNase* candidates. PCR was carried out using specific primers detailed in Table S1. *S-RNase* candidates assayed are indicated at the *left* of each panel. **a** RT-PCR analysis of style transcripts from NaM individuals. **b** Genomic PCR analysis in different *S*-genotypes from a *Nicotiana alata* laboratory population. **c** Genomic PCR analysis in *Nicotiana longiflora* and a self-compatible accession of *Nicotiana alata* (cv Breakthrough). Controls, DNA template with (+) and without (−) the sequence of the assayed *S-RNase* candidate

earliest stage analyzed; then it increased gradually to reach their maximum level close to maturity, when styles are fully capable of pollen rejection, near the anthesis stage. Immediately after anthesis, the expression remained constant or slightly decreased. However, S_{63} ribonuclease showed a stable amplification during all developmental bud stages, with clear early expression in the first stage of style development analyzed. These results indicate that the non-S_{63}-*RNase* is a constitutive and ubiquitous ribonuclease whose function appears to be not restricted to the reproductive process. The spatial and developmental expression of S_{75}- and S_{210}-*RNase* candidates was similar to the pattern showed by S_{c10}-*RNase* and the *S-RNase* candidates in Fig. 3a, b (Supplementary Fig. S4).

Functionality of novel putative *S-RNase* alleles

Functionality of SI was tested for all putative *S-RNases* identified. The two more frequent *S-RNase* candidates in NaM individuals, S_5 and S_{107}, were tested first. These genes showed the typical expression of an *S-RNase* in different tissues and style developmental stages (Fig. 3), suggesting they could be functional in SI. To test S_5 and S_{107} functionality, allele-specific PCR was performed in the progeny of the half-compatible cross NaM-3 × NaM-6 (Table 1). From the results of Fig. 2a, NaM-3 showed three *S*-allele candidates (S_5, S_{27}, and S_{107}) while NaM-6 showed two candidates (S_5 and S_{107}). The progeny segregation of the S_{107}-*RNase* candidate fitted the expected 1:1 ratio,

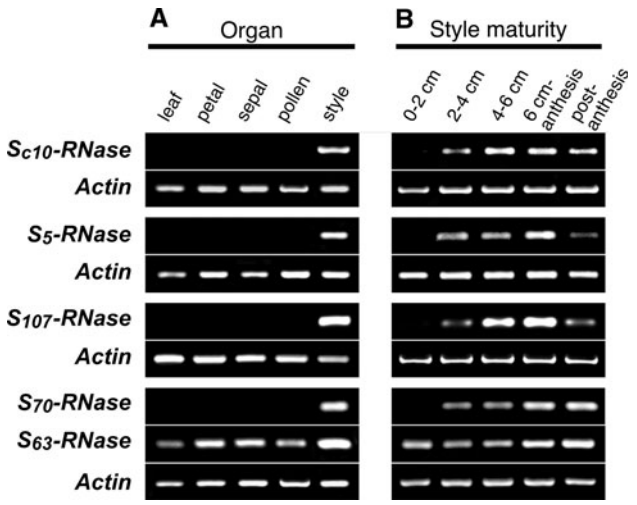

Fig. 3 RT-PCR analysis of transcripts of *S-RNase* candidates. PCR was carried out using allele-specific primers shown in Table S1. **a** Organ-specificity, **b** style developmental stages. 32 PCR cycles were performed for all transcripts assayed. Actin was used as positive control on each preparation of total RNA

indicating that the presence of this candidate is only due to maternal contribution and confirming that it is a functional *S-RNase* allele. However, the progeny segregation of S_5*-RNase* candidate rejected the 1:1 ratio, indicating that it was not a functional allele of *S-RNase* in the NaM population. As expected, all progeny derived from the cross NaM-3 × NaM-6 bore the non-functional S_{63} ribonuclease (result not shown).

Similar analysis was conducted on the other *S-RNase* candidates identified from the NaM population (Table 2). In this case, the single compatible paternal allele expected in the progeny of parents sharing one common *S*-allele was tested. Because S_5 ribonuclease was ruled out as an *S-RNase* allele (Table 1), in the crosses shown in Table 2 each parent has only two *S-RNase* allele candidates. The crosses to test functionality of the putative S_{75}-, S_{70}-, and S_{27}*-RNases* demonstrated that these alleles are fully functional *S*-haplotypes, since the hypothesis of full compatible crosses was rejected in each case (Table 2). Besides doing control crosses to show paternal segregation of functional S_{107}- and S_{c10}*-RNases,* a full compatible cross between parents not sharing a common allele (NaM-3 × NaM-5) was performed as an additional control. As expected, progeny segregation fits 1:1 ratio indicating that in this case the pollen contribution is not restricted to a single *S*-allele.

The S_{210}*-RNase* candidate also appears to be a functional *S*-allele, although some leakiness was observed in the cross performed to evaluate this *S*-allele. The genotypes of the three individuals not bearing the paternal allele S_{c10} (Table 2, cross NaM-12 × NaM-2) were $S_{107}S_{210}$, confirming that 15% of assessed progeny was derived from pollen tubes bearing the S_{210} haplotype that escaped rejection (Supplementary Fig. S5, progeny r, s, and t from cross NaM-12 × NaM-2). The complete segregation of *S*-genotypes from three selected crosses of Table 2 is also shown in Supplementary Fig. S5. In each cross, the novel *S-RNase* candidates segregated with each other, as expected for functional *S-RNases* of the *S*-locus.

Phylogenetic analysis

Phylogenetic analysis was conducted to determine evolutionary relationships and the extent of polymorphism among the *S-RNase* sequences from *N. alata* and five other species of Solanaceae. In previous phylogenetic analysis, *S*-alleles of *N. alata* appeared to be distributed into few *S*-lineages, compared to other species of SI solanaceae sampled more extensively (Richman and Kohn 2000). Posterior probabilities and bootstrap values derived from Bayesian inference (BI) and maximum-likelihood (ML) analysis provided strong support for almost all non-basal nodes of the tree (Fig. 4). Eight transgeneric (TG) *S*-lineages were identified for *N. alata S-RNases* (including the *non-S-RNases*), defined as the most recent nodes including *S*-alleles from more than one species (designated I–VIII in Fig. 4). TG lineages II and III concentrated four and three *S-RNases*, respectively, while the novel *S-RNases* identified in this work were distributed in five out of eight TG lineages. Given the strong support values of the single leaf node containing S_{27}*-RNase*, it was considered an independent TG lineage; its isolation could be due to incomplete sampling of *S-RNase* polymorphism or rapid divergence from its ancestral lineage.

Table 1 Segregation of S_5- and S_{107}*-RNase* candidates to test SI functionality

S-RNase candidates of NaM parents[a]	Family size	Candidate tested	Observed ratio (+:−)	Expected ratio (+:−)[b]	X^2 (*P* value)
3 (S_5, S_{107}, S_{27}) × 6 (S_5, S_{107}, $S_?$)	34	S_5	34:0	1:1	34 (<0.0001)
		S_{107}	16:18	1:1	0.12 (0.73)

+:− presence or absence of the *S-RNase* candidate tested for functionality

[a] The *S-RNase* candidates of NaM parents are based on Fig. 2a

[b] Expected ratio if the shared *S-RNase* candidate tested is fully functional in SI

Table 2 Segregation of pollen-derived *S*-allele in semi-compatible crosses to test SI functionality

NaM parents (proposed *S*-genotype)[a,b]	Family size	Allele tested	Paternal allele assayed by PCR	Observed ratio (+:−)	Expected ratio (+:−)[c]	X^2 (*P* value)
5 ($S_{70}S_{75}$) × t_1 ($S_{c10}S_{75}$)	28	S_{75}	S_{c10}	28:0	1:1	28 (<0.0001)
5 ($S_{70}S_{75}$) × t_2($S_{c10}S_{70}$)	20	S_{70}	S_{c10}	20:0	1:1	20 (<0.0001)
3 ($S_{107}S_{27}$) × 7 ($S_{c10}S_{107}$)	20	S_{107}	S_{c10}	20:0	1:1	20 (<0.0001)
12 ($S_{107}S_{210}$) × 2 ($S_{c10}S_{210}$)	20	S_{210}	S_{c10}	17:3	1:1	9.8 (<0.0017)
10 ($S_?S_{27}$) × 3 ($S_{107}S_{27}$)	18	S_{27}	S_{107}	18:0	1:1	18 (<0.0001)
t_1 ($S_{c10}S_{75}$) × t_2 ($S_{c10}S_{70}$)	20	S_{c10}	S_{70}	20:0	1:1	20 (<0.0001)
3 ($S_{27}S_{107}$) × 5 ($S_{70}S_{75}$)[d]	17	–	S_{75}	8:9	1:1	0.059 (0.812)

+:− presence or absence of the paternal allele assayed by PCR

[a] The proposed *S*-genotype of NaM parents is based on results shown in Fig. 2a and Table 1

[b] t_1 and t_2 are tester plants bearing the *S*-allele *S_{c10}-RNase*

[c] Expected ratio if the shared, putative *S*-allele is non-functional and the cross is fully compatible

[d] Control, fully compatible cross

Ten rooted clades (labeled 1–10), derived from ancestral nodes with solid bootstrap and posterior probabilities values, were also identified in the tree of Fig. 4. With a few exceptions, *S-RNases* from *N. alata*, *Petunia inflata*, *Lycium parishii* and *Solanum chilense* cluster together and are broadly distributed in clades 1–10. In contrast, *Witheringia solanacea* and *Physalis longifolia* are clearly restricted to three clades (3, 8, and 10). The small number of ancient *S*-lineages covered by alleles from these species is in agreement with several previous reports (Richman and Kohn 2000; Stone and Pierce 2005; Savage and Miller 2006; Lu 2006).

Discussion

Identification of cDNAs encoding *S-RNases* from a natural population of *Nicotiana alata*

This work reports the identification, expression analysis, functional characterization, and phylogenetic origin of *S-RNase* alleles from a natural population of the self-incompatible species *N. alata*. Several natural populations of Solanaceae have been surveyed for *S-RNase* alleles using RT-PCR techniques (Tsukamoto et al. 1999; Igic et al. 2007 and references therein; Mena-Alí and Stephenson 2007). However, despite the early use of *N. alata* to explore the genetic diversity of SI (East and Yarnell 1929) and the extensive research conducted to understand the complex molecular basis of S-RNase-based SI (reviewed in McClure 2008), no examination of *S-RNase* diversity at the molecular level has been reported from natural populations of this species. Consequently, the number of reported *S-RNase* alleles of *N. alata* in databanks is limited compared to other self-incompatible solanaceous species.

Degenerate primers based on conserved domains C1 and C5 were effective for amplifying *N. alata S-RNases*. Overall, ten different *S-RNase* candidate sequences of approximately 500 bp were identified (Supplementary Table S2). Three sequences (*S_2, S_6, and S_{c10}*) were well-documented *S-RNase* alleles involved in SI (Anderson et al. 1989; Murfett et al. 1996). Another *S-RNase* candidate sequence, designated S_{63} in this work, was very similar to *N. alata* pistil ribonuclease MS1 (Kuroda et al. 1994). The remaining six sequences (*S_5-, S_{27}-, S_{70}-, S_{75}-, S_{107}-,* and *S_{210}-RNases*) represented new *N. alata S*-haplotype candidates, not previously reported. The alignment of deduced amino acid sequences of these putative S-RNases with S_{c10}-RNase, showed the typical primary structure of solanaceous S-RNases (Fig. 1).

Although two different *S-RNases* from the *S*-locus are expected in plants displaying S-RNase-based SI, in some individuals only a single *S-RNase* candidate was identified, while in others, more than two *S-RNase* candidates were recovered (Supplementary Table S2). In the first case, the differential affinity of degenerate primers could largely favor the amplification of a single sequence. Another possible explanation could be a significantly different transcript level or stability between the two *S-RNase* alleles expected for the *S*-locus. Alternatively, style expression of *S-like RNases* or relic *S-RNases,* which structurally resemble functional *S-RNases*, could explain the amplification of more than two sequences related to *S-RNases* in each individual.

The high frequency of S_{63} and S_5 sequences among the NaM individuals screened suggested that these alleles could represent in fact *S-like RNases* or relic *S-RNases*. The proteins encoded by these genes are members of the S-RNase super family (Green 1994) and have been reported in both self-compatible and self-incompatible species of many plant

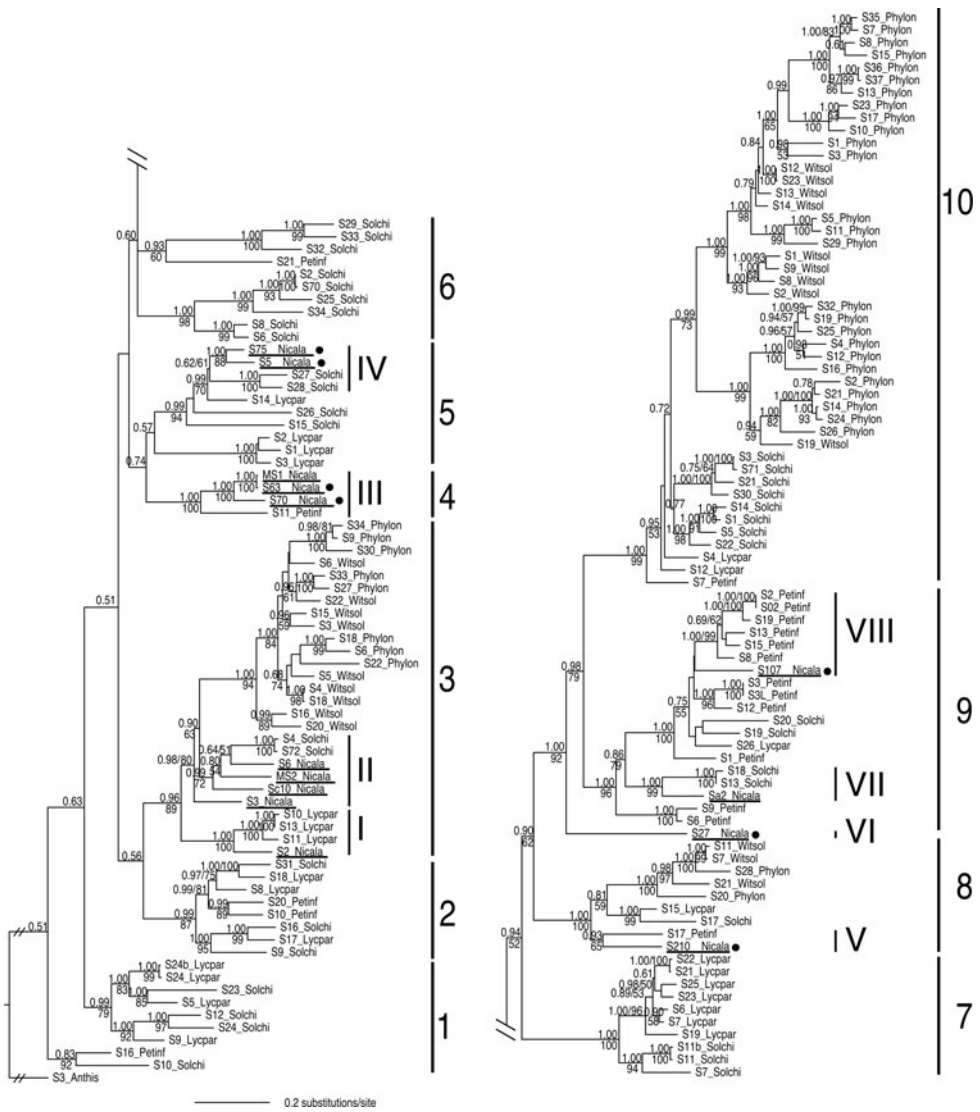

Fig. 4 Phylogenetic analysis of *S-RNases* from the Solanaceae. Maximum-likelihood tree topology depicting phylogenetic relationships of *S-RNases* from *Nicotiana alata* (Nical), *Petunia inflata* (Petinf), *Solanum chilense* (Solchi), *Lycium parishii* (Lycpar), *Physalis longifolia* (Phylon) and *Witheringia solanacea* (Witsol). Eight *Nicotiana alata* TG lineages (lines I–VIII) and ten ancient *S*-lineages (lines 1–10) are shown. *Nicotiana alata* alleles are *underlined*, and novel *S-RNases* reported in this work are highlighted with a *black dot*. Posterior probabilities and bootstrap values (percentage of 1,000 bootstrap replica) are shown for corresponding nodes when their value exceeds 50%. The tree was rooted with S_3*-RNase* from *Antirrhinum hispanicum* (Anthis). Accession numbers for the 154 *S-RNase* alleles used are in the supplementary File S1

families. *S-like RNases* are not linked to *S*-locus; their expression is not restricted to the pistil and the corresponding proteins usually exhibit several conserved residues between C1 and C3 domains that are not conserved in S-RNases. Frequently, their functions are related to stress scenarios, like phosphate starvation or pathogen attack (Dodds et al. 1996; Hugot et al. 2002). Relic *S-RNases* genes are a particular type of *S-like RNases*, they are not linked to *S*-locus either and their expression is restricted to the pistil. Originally they were described in SC species (Golz et al. 1998) although they have been also reported in SI species (Lee et al. 1992; Liang et al. 2003). So far, no particular role has been assigned to relic *S-RNases* and probably, they originated as paralogous copies of functional *S-RNases*. Phylogenetic analysis has shown that relic *S-RNases* and functional *S-RNases* share the same origin, while *S-like RNases* are more distantly related genes that group in an independent clade (Golz et al. 1998; Liang et al. 2003).

Neither S_{63} nor S_5 amino acid sequences were significantly different from the rest of the S-alleles aligned in Fig. 1. Moreover, the highest identities among the S-RNase candidates were found between the S_{63} and S_{70} and between the S_5 and S_{75}. In contrast to the high frequency of S_{63} and S_5, S_{70} and S_{75} were expressed in only two and three individuals of the NaM population, respectively (Fig. 2; Supplementary Fig. S2). The close structural resemblance between *S-RNases*, *S-like RNases*, and relic *S-RNases* means that functional and expression analyses are required to determine which candidates are truly *S-RNase* alleles.

Expression and functionality of *N. alata* style *S-RNases*

Due to the high divergence of HV regions among *S-RNase* alleles, PCR with specific primers based on HVa/HVb regions has been extensively used for genotyping the *S*-locus in self-incompatible species. RT-PCR conducted

with specific primers showed individual-specific expression in the NaM population for all the new *S-RNase* candidates, except the S_{63} gene. This pattern of expression was the one expected for *S*-alleles involved in SI (Fig. 2). In contrast, S_{63} was the only sequence detected in all the plants examined, a trait consistent with a *non-S-RNase*. The specificity of putative *S-RNases* was further assayed in different organs and in developing styles, using S_{c10}*-RNase* as an internal control (Fig. 3). Again, all the *S-RNase* candidates analyzed but S_{63}, mimicked both S_{c10}*-RNase* spatial and temporal patterns of expression. The RT-PCR analysis of S_{c10}*-RNase* transcript in developing styles was almost identical to the expression of this *S*-allele previously assessed by RNA gel-blot analysis (McClure et al. 1999). Thus, the primary structure, the individual-specific expression and the spatial and temporal expression patterns of *S-RNase* candidates were the ones expected for *S-RNases* involved in SI. Conversely, the ubiquitous expression of S_{63} ribonuclease, both in different individuals and tissues, precluded it from encoding the specificity factor in the SI reaction and suggested that its role is not restricted to the reproductive process only.

To test whether the sequences of putative *S*-alleles were associated with SI phenotypes, the progeny of half-compatible crosses was analyzed (Tables 1, 2). All sequences assayed, except S_5 and S_{63}, showed that the *S-RNase* candidates were functional in the SI reaction. Thus, S_{70}-, S_{75}-, S_{27}-, S_{107}-, and S_{210}*-RNases* are novel functional *S*-haplotypes of *N. alata*. The minor leakiness observed in the S_{210}*-RNase* test cross was not unusual in natural populations of solanaceous species as we discuss below. Therefore, based on RT-PCR genotyping shown in Fig. 2 and the functionality tests of Tables 1 and 2, the *S*-genotype proposed for the 12 NaM individuals analyzed in this work is shown in Table 3. One *S*-haplotype of each of plants 1, 6, and 10 still remain unknown.

Both S_5 and S_{63} alleles were *non-S-RNases* similar to relic *S-RNases*, regarding their deduced amino acid sequence (indistinguishable from S-RNases), their failure in pollen rejection, and their phylogenetic origin, shared with functional *S-RNases* but different from *S-like-RNases* (Fig. 1; Table 1; Supplementary Fig. S6). However, the pattern of relative expression in different organs was different for these two genes. While the non-functional S_5*-RNase* showed the organ expression of a relic *S-RNase*, typically restricted to the style, the non-functional S_{63}*-RNase* expression was ubiquitous and it resembled that of *S-like-RNases.* It will be interesting to know if these two genes are also related to nutritional metabolism or response to pathogen attack, as was previously established for *S-like-RNases* (Dodds et al. 1996; Hugot et al. 2002; Liang et al. 2002). It is intriguing that these two *non-S-RNase*s, S_{63} and S_5, are highly similar to other two functional S-RNases, exhibiting identity values higher than those of *Nicotiana* S-RNase alleles (Supplementary Fig. S2). S_{63} appears to have diverged from S_{70} before S_5 diverged from S_{75}, since S_{63} ubiquity and presence in SC *Nicotiana* species, suggested that S_{63} had diverged before *Nicotiana* speciation (Fig. 2c).

Table 3 *S*-genotype of NaM individuals

NaM individuals	*S*-genotype[a]
1	$S_{75}S_?$
2	$S_{c10}S_{210}$
3	$S_{27}S_{107}$
4	$S_{75}S_6$
5	$S_{75}S_{70}$
6	$S_{107}S_?$
7	$S_{c10}S_{107}$
8	$S_{27}S_{107}$
9	S_2S_{107}
10	$S_{27}S_?$
11	$S_{70}S_{107}$
12	$S_{210}S_{107}$

[a] The *S*-genotype was inferred from results of Fig. 2a and Tables 1 and 2

Genealogy of novel *S-RNase* haplotypes

To analyze the phylogeny of *N. alata S-RNases*, five GSI species of the Solanaceae with distinct patterns of *S-RNase* allele evolution were chosen: *S-RNases* from *Solanum chilense*, *Lycium parishii*, and *Petunia inflata* were shown to represent a broad sample of ancient *S*-allele lineages (Igic et al. 2007; Savage and Miller 2006; Wang et al. 2001) while *Physalis longifolia*, and *Witheringia solanacea S-RNases* were grouped in clusters in a small subset of transgeneric *S*-lineages (Lu 2006; Stone and Pierce 2005). In the tree shown in Fig. 4, *Petunia*, *Lycium*, *Solanum*, and *Nicotiana S-RNases* tended, in general, to group together without relevant clustering in species-specific subgroups. To our knowledge, *S-RNase* diversity has been surveyed only in one natural population of *N. alata* (this work) and *P. inflata* (Wang et al. 2001). Both species exhibited the lowest number of *S-RNase* alleles from the species included in this study. Therefore, incomplete sampling would explain the absence of *S*-alleles from *P. inflata* in clades 3, 5, and 7 and from *N. alata* in clades 1, 2, 6, and 7.

Overall, the *S-RNase* phylogenetic pattern showed that *N. alata* displays a broad sample of the allelic variation at the *S*-locus of the Solanaceae. As was previously pointed out, the close clustering of species from SI Solanaceae shows that the most extant diversity of *S-RNases* represents an ancient *S-RNase* polymorphism that appears to predate

the divergence of the species (Ioerger et al. 1990; Richman and Kohn 2000).

The functional analysis of the novel *S-RNases* described in this work revealed, in general, a robust SI response. Such behavior has been found previously in natural populations. For instance, a sample of ten new *S-RNases* identified from a natural population of wild tomato *Solanum chilense* exhibited a tight SI mechanism (Igic et al. 2007). However, solanaceous species from natural populations have shown a marked phenotypic variation in the strength of SI reaction. Often, natural populations display a mixture of self-compatible and self-incompatible individuals, including intermediate behaviors with diverse degree of self-fertilization tendency (Tsukamoto et al. 1999; Stone et al. 2006). Then, the importance of examining SI in these populations is based on the high level of diversity they may exhibit in the expression of SI response. This natural variation is caused by different mechanisms such as deficient S-RNase expression or function (Tsukamoto et al. 2003a; Mena-Alí and Stephenson 2007), or loss of pollen function (Tsukamoto et al. 2003b). Pollen rejection in S-RNase-based SI is a complex mechanism involving the recruitment of several proteins other than the specificity factors of locus *S*. In *N. alata* and other solanaceous species, *trans*-acting stylar factors are required for SI (McClure et al. 1999; O'Brien et al. 2002; Hancock et al. 2005; Puerta et al. 2009). Other putative factors have been proposed as part of the molecular machinery that leads to pollen rejection (Goldraij et al. 2006; Hua and Kao 2006; McClure 2008). Currently individuals in the NaM population showing low or null ability for self-pollen rejection are being selected. The analysis of these individuals, possibly deficient in factor/s involved in pollen rejection, will contribute to elucidate the complex molecular mechanism of S-RNase-based SI.

Acknowledgments We thank Dr Bruce McClure, Dr Jorge Muschietti, and Dr Carlos Argaraña for critical reading of the manuscript; Dr Andrew Jackson for advice and discussion regarding phylogenetic issues, and Dr María E Alvarez for helpful discussions. We thank Gabriela Díaz Cortez for editorial assistance. This work was funded by grants of Agencia Nacional de Promoción Científica y Tecnológica (PICT 05/32933) and SECyT-Universidad Nacional de Córdoba to Ariel Goldraij.

References

Anderson AG, McFadden I, Bernatzky R, Atkinson A, Orpin T et al (1989) Sequence variability of three alleles of the self-incompatibility gene of *Nicotiana alata*. Plant Cell 1:483–491

de Nettancourt D (2001) Incompatibility and incongruity in wild and cultivated plants. Springer, Berlin

Dodds PN, Clarke AE, Newbigin E (1996) Molecular characterisation of an S-like RNase of *Nicotiana alata* that is induced by phosphate starvation. Plant Mol Biol 31:227–238

East E, Yarnell SH (1929) Studies on self-sterility VIII. Self-sterility allelomorphs. Genetics 14:455–487

Goldraij A, Kondo K, Lee CB, Hancock CN, Sivaguru M, Vázquez-Santana S, Kim S, Phillips TE, Cruz-García F, McClure BA (2006) S-RNase compartmentalization and HT-B degradation in self-incompatible *Nicotiana*. Nature 439:805–810

Golz JF, Clarke AE, Newbigin E, Anderson M (1998) A relic S-RNase is expressed in the styles of self-compatible *Nicotiana sylvestris*. The Plant J 16:591–599

Goodspeed TH (1954) The genus *Nicotiana*. Origins, relationships and evolution of its species in the light of their distribution, morphology and cytogenetics. Chronica Botanica Company, Waltham, MA, pp 389–405

Green PJ (1994) The ribonucleases of higher plants. Ann Rev of Plant Physiol Plant Mol Biol 45:421–445

Hancock CN, Kent L, McClure B (2005) The stylar 120 k glycoprotein is required for S-specific pollen rejection in *Nicotiana*. Plant J 43:716–723

Hauck NR, Yamane H, Tao R, Iezzoni AF (2006) Accumulation of non-functional *S*-haplotypes results in the breakdown of gametophytic self-incompatibility in tetraploid *Prunus*. Genetics 172:1191–1198

Hua Z, Kao T-h (2006) Identification and characterization of components of a putative *Petunia S*-locus F-box-containing E3 ligase complex involved in S-RNase-based self-incompatibility. Plant Cell 18:2531–2553

Huang S, Lee HS, Karunandaa B, Kao T-h (1994) Ribonuclease activity of *Petunia inflata S* proteins is essential for rejection of self-pollen. Plant Cell 6:1021–1028

Hugot K, Ponchet M, Marais A, Ricci P, Galiana E (2002) A tobacco S-like RNase inhibits hyphal elongation of plant pathogens. Mol Plant Microbe Int 15:243–250

Igic B, Smith WA, Robertson KA, Schaal BA, Kohn JR (2007) Studies of self-incompatibility in wild tomatoes: I. S-allele diversity in *Solanum chilense* Dun. (Solanaceae). Heredity 99:553–561

Ioerger TR, Clarke AE, Kao T-h (1990) Polymorphism at the self-incompatibility locus in Solanaceae predates speciation. Proc Nat Acad Sci USA 87:9732–9735

Ioerger TR, Gohlke JR, Xu B, Kao T-h (1991) Primary structural features of the self-incompatibility protein in Solanaceae. Sex Plant Reprod 4:81–87

Ippolito A, Fernandes GW, Holtsford TP (2004) Pollinator preferences for *Nicotiana alata*, *N. forgetiana*, and their *F1* hybrids. Evolution 58:2634–2644

Kao T-h, Tsukamoto T (2004) The molecular and genetic bases of S-RNase-based self-incompatibility. Plant Cell 16:S72–S83

Kokubun H, Nakano M, Tsukamoto T, Watanabe H, Hashimoto G, Marchesi E, Bullrich L, Basualdo IL, Kao TH, Ando T (2006) Distribution of self-compatible and self-incompatible populations of *Petunia axillaris* (Solanaceae) outside Uruguay. J Plant Res 5:419–430

Kuroda S, Norioka S, Mitta M, Kato I, Sakiyama F (1994) Primary structure of a novel stylar RNase unassociated with self-incompatibility in tobacco plant *Nicotiana alata*. J Prot Chem 13:438–439

Lee HS, Singh A, Kao T-h (1992) RNase X2, a pistil-specific ribonuclease from *Petunia inflata,* shares sequence similarity with solanaceous S proteins. Plant Mol Biol 20:1131–1141

Lee HS, Huang S, Kao T-h (1994) S proteins control rejection of incompatible pollen in *Petunia inflata*. Nature 367:560–563

Lee CB, Page LE, McClure BA, Holtsford TP (2008) Post-pollination hybridization barriers in *Nicotiana* section Alatae. Sex Plant Reprod 21:183–195

Liang L, Lai Z, Ma W, Zhang Y, Xue Y (2002) *AhSL28*, a senescence- and phosphate starvation-induced S-like RNase gene in *Antirrhinum*. Biochem Biophys Acta 17:5964–5971

Liang L, Huang J, Xue Y (2003) Identification and evolutionary analysis of a relic S-RNase in *Antirrhinum*. Sex Plant Reprod 16:17–22

Lu Y (2006) Historical events and allelic polymorphism at the gametophytic self-incompatibility locus in Solanaceae. Heredity 96:22–28

Luu DT, Qin XK, Morse D, Capadoccia M (2000) S-RNase uptake by compatible pollen tubes in gametophytic self-incompatibility. Nature 407:649–651

Matton DP, Maes C, Laublin G, Qin XK, Bertrand C, Morse D, Cappadoccia M (1997) Hypervariable domains of self-incompatibility RNases mediate allele-specific pollen recognition. Plant Cell 9:1757–1766

McClure BA (2008) Comparing models for S-RNase-based self-incompatibility. In: Franklin-Tong VE (ed) Self-incompatibility in flowering plants. Evolution diversity and mechanisms. Springer, Berlin, pp 217–236

McClure BA (2009) Darwin foundation for investigating self-incompatibility and the progress toward a physiological model for S-RNase-based SI. J Exp Bot 60:1069–1081

McClure BA, Haring V, Ebert PR, Anderson MA, Simpson RJ, Sakiyama F, Clarke AE (1989) Style self-incompatibility gene products of *Nicotiana alata* are ribonucleases. Nature 342:955–957

McClure BA, Gray JE, Anderson MA, Clarke AE (1990) Self-incompatibility in *Nicotiana alata* involves degradation of pollen rRNA. Nature 347:757–760

McClure BA, Mou B, Canevascini S, Bernatzky R (1999) A small asparagine-rich protein required for S-allele specific pollen rejection in *Nicotiana*. Proc Nat Acad Sci USA 96:13548–13553

McClure BA, Cruz-García F, Beecher B, Sulaman W (2000) Factors affecting inter- and intra-specific pollen rejection in *Nicotiana*. Ann Bot 85:113–123

Mena-Alí JI, Stephenson AG (2007) Segregation analyses of partial self-incompatibility in self and cross progeny of *Solanum carolinense* reveal a leaky S-allele. Genetics 177:501–510

Miller JS, Levin RA, Feliciano NM (2008) A tale of two continents: Baker's rule and the maintenance of self-incompatibility in *Lycium* (Solanaceae). Evolution 5:1052–1065

Murfett J, Atherton TL, Mou B, Gasser CS, McClure BA (1994) S-RNase expressed in transgenic *Nicotiana* causes S-allele-specific pollen rejection. Nature 367:563–566

Murfett J, Strabala TJ, Zurek DM, Mou B, Beecher B, McClure BA (1996) S-RNase and interspecific pollen rejection in the genus *Nicotiana*: multiple pollen-rejection pathways contribute to unilateral incompatibility between self-incompatible and self-compatible species. Plant Cell 8:943–958

O'Brien M, Kapfer C, Major G, Laurin M, Bertrand C, Kondo K, Kowyama Y, Matton DP (2002) Molecular analysis of the stylar-expressed *Solanum chacoense* asparagine-rich protein family related to the HT modifier gametophytic self-incompatibility in *Nicotiana*. The Plant J 32:1–12

Pandey KK (1979) The genus *Nicotiana*: evolution of incompatibility in flowering plants. In: Hawkes JG, Lester RN, Skelding AD (eds) The biology and taxonomy of the Solanaceae. Academic, London

Puerta AR, Ushijima K, Koba T, Sassa H (2009) Identification and functional analysis of pistil self-incompatibility factor *HT-B* of *Petunia*. J Exp Bot 60:1309–1318

Richman A, Kohn JR (2000) Evolutionary genetics of self-incompatibility in the Solanaceae. Plant Mol Biol 42:169–179

Richman A, Kao T-h, Schaeffer SW, Uyenoyama MK (1995) S-allele sequence diversity in natural populations of *Solanum carolinense* (Horsenettle). Heredity 75:405–415

Richman AD, Uyenoyama MK, Kohn JR (1996) S-allele diversity in a natural population of *Physalis crassifolia* (Solanaceae) (ground cherry) assessed by RT-PCR. Heredity 76:497–505

Ronquist F, Huelsenbeck JP (2003) MRBAYES 3: Bayesian phylogenetic inference under mixed models. Bioinformatics 19:1572–1574

Savage AE, Miller JS (2006) Gametophytic self-incompatibility in *Lycium parishii* (Solanaceae): allelic diversity, genealogical structure and patterns of molecular evolution. Heredity 96:434–444

Sijacic P, Wang X, Skirpan L, Wang Y, Dowd PE, McCubbin AG, Huang S, Kao T-h (2004) Identification of the pollen determinant of S-RNase-mediated self-incompatibility. Nature 429:302–305

Stamatakis A (2006) RAxML-VI-HPC: maximum likelihood-based phylogenetic analyses with thousands of taxa and mixed models. Bioinformatics 22:2688–2690

Stamatakis A, Hoover P, Rougemont J (2008) A rapid bootstrap algorithm for the RaxML web servers. Syst Biol 57:758–771

Stone JL, Pierce S (2005) Rapid recent radiation of S-RNase lineages in *Whiteringia solanaceae* (Solanaceae). Heredity 94:547–555

Stone JL, Sasuclark MA, Blomberg C (2006) Variation in the self-incompatibility response within and among populations of the tropical shrub *Witheringia solanaceae* (Solanaceae). Am J Bot 93:592–598

Thompson JD, Gibson TJ, Plewniak F, Jeanmouguin F, Higgins DG (1997) The ClustalX window interface: flexible strategies for multiple sequence alignment aided by quality analysis tools. Nucleic Acid Res 24:4876–4882

Tsukamoto T, Ando T, Kokubun H, Watanabe H, Masada M, Zhu X, Marchesi E, T-h Kao (1999) Breakdown of self-incompatibility in a natural population of *Petunia axillaris* (Solanaceae) in Uruguay containing both self-incompatible and self-compatible plants. Sexual Plant Reprod 12:6–13

Tsukamoto T, Ando T, Kokubun H, Watanabe H, Sato T, Masada M, Marchesi E, Kao T-h (2003a) Breakdown of self-incompatibility in a natural population of *Petunia axillaris* caused by a modifier locus that suppresses the expression of an S-RNAse gene. Sexual Plant Reprod 15:255–263

Tsukamoto T, Ando T, Takahashi K, Omori T, Watanabe H, Kokubun H, Marchesi E, Kao T-h (2003b) Breakdown of self-incompatibility in a natural population of *Petunia axillaris* caused by loss of pollen function. Plant Physiol 131:1903–1912

Tsukamoto T, Potter V, Tao R, Vieira CP, Vieira J, Iezzoni AF (2008) Genetic and molecular characterization of three novel *S*-haplotypes in sour cherry (*Prunus cerasus* L.). J Exp Bot 59:3169–3185

Wang X, Tsukamoto T, Ando T, Kao T-h (2001) Evidence that intragenic recombination contributes to allelic diversity of the S-RNase gene at the self-incompatibility (S) locus in *Petunia inflata*. Plant Physiol 125:1012–1022

Wheeler D, Newbigin E (2007) Expression of 10 S-Class *SLF-like* genes in *Nicotiana alata* pollen and its implications for understanding the pollen factor of the S locus. Genetics 177:2171–2180